Accepted Manuscript

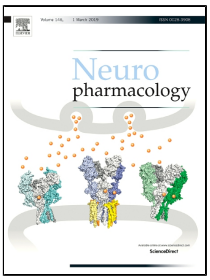

GABA$_A$R isoform and subunit structural motifs determine synaptic and extrasynaptic receptor localisation

Saad Hannan, Marielle Minere, Joseph Harris, Pablo Izquierdo, Philip Thomas, Becky Tench, Trevor G. Smart

PII:	S0028-3908(19)30056-5
DOI:	10.1016/j.neuropharm.2019.02.022
Reference:	NP 7540
To appear in:	*Neuropharmacology*
Received Date:	12 November 2018
Accepted Date:	14 February 2019

Please cite this article as: Saad Hannan, Marielle Minere, Joseph Harris, Pablo Izquierdo, Philip Thomas, Becky Tench, Trevor G. Smart, GABA$_A$R isoform and subunit structural motifs determine synaptic and extrasynaptic receptor localisation, *Neuropharmacology* (2019), doi: 10.1016/j.neuropharm.2019.02.022

$GABA_AR$ isoform and subunit structural motifs determine synaptic and extrasynaptic receptor localisation

Saad Hannan, Marielle Minere, Joseph Harris[1], Pablo Izquierdo,

Philip Thomas, Becky Tench[2] and Trevor G. Smart*

Department of Neuroscience, Physiology and Pharmacology

University College London

Gower Street

London WC1E 6BT, UK

*Correspondence to: t.smart@ucl.ac.uk

[1]Present address: North Middlesex University Hospital, Sterling Way, London N18 1QX

[2]Present address: School of Physiology, Pharmacology and Neuroscience, University of Bristol, University Walk, Bristol BS8 1TD, UK

Abstract

$GABA_A$ receptors ($GABA_ARs$) are the principal inhibitory neurotransmitter receptors in the central nervous system. They control neuronal excitability by synaptic and tonic forms of inhibition mostly mediated by different receptor subtypes located in specific cell membrane subdomains. A consensus suggests that α1-3βγ comprise synaptic $GABA_ARs$, whilst extrasynaptic α4βδ, α5βγ and αβ isoforms largely underlie tonic inhibition. Although some structural features that enable the spatial segregation of receptors are known, the mobility of key synaptic and extrasynaptic $GABA_ARs$ are less understood, and yet this is a key determinant of the efficacy of GABA inhibition. To address this aspect, we have incorporated functionally silent α-bungarotoxin binding sites (BBS) into prominent hippocampal $GABA_AR$ subunits which meidate synaptic and tonic inhibition. Using single particle tracking with quantum dots we demonstrate that $GABA_ARs$ that are traditionally considered to mediate synaptic or tonic inhibition are all able to access inhibitory synapses. These isoforms have variable diffusion rates and are differentially retained upon entering the synaptic membrane subdomain. Interestingly, α2 and α4 subunits reside longer at synapses compared to α5 and δ subunits. Furthermore, a high proportion of extrasynaptic δ-containing receptors exhibited slower diffusion compared to δ subunits at synapses. A chimera formed from δ-subunits, with the intracellular domain of γ2L, reversed this behaviour. In addition, we observed that receptor activation affected the diffusion of extrasynaptic, but not of synaptic $GABA_ARs$. Overall, we conclude that the differential mobility profiles of key synaptic and extrasynaptic $GABA_ARs$ are determined by receptor subunit composition and intracellular structural motifs.

Words – 248

Highlights

1. $GABA_AR$s mediating synaptic or tonic inhibition all access inhibitory synapses
2. Diffusion and retention of $GABA_AR$s at synapses depends on the subunit composition
3. Dwell times for α2 and α4 are longer than for α5 and δ at inhibitory synapses
4. A large proportion of extrasynaptic δ-$GABA_AR$s exhibit restricted diffusion
5. The large intracellular loops of δ and γ2L regulate mobility and synaptic trapping

1. Introduction

γ-aminobutyric acid type-A receptors ($GABA_A$Rs) form part of the pentameric ligand-gated ion channel family and are the main inhibitory neurotransmitter receptors in the central nervous system (Smart, 2015; Luscher et al., 2011). These receptors are crucial for maintaining control over excitability and neural network computation (Klausberger et al., 2002) and their dysfunction is associated with several neurological conditions including: epilepsy (Oyrer et al., 2018; Macdonald et al., 2010), cognitive impairment (Rudolph and Mohler, 2014), and schizophrenia (Braat and Kooy, 2015; Schmidt and Mirnics, 2015). $GABA_A$Rs mediate two distinct types of inhibition in the brain: phasic and tonic. Phasic inhibition is brief in duration (typically milliseconds) and arises due to release of GABA from presynaptic interneurons. Activation of postsynaptic $GABA_A$Rs briefly hyperpolarises and electrically shunts the neuronal membrane to regulate excitability (Mitchell and Silver, 2003). In contrast, tonic inhibition arises due to the persistent background activity of $GABA_A$Rs in response to ambient and synaptic GABA spillover (Glykys and Mody, 2007). Tonic inhibition exerts a persistent control over neuronal excitability and is important for setting the gain for spike firing (Mitchell and Silver, 2003).

$GABA_A$Rs are assembled from 19 subunits (α1–6, β1–3, γ1–3, δ, ρ1–3, ε, π, and θ) and the prototypical pentamer consists of 2α, 2β and a γ/δ subunits (Sieghart and Sperk, 2002). Even though such a large number of subunits can generate considerable diversity for receptor subtypes, interestingly, only certain subunit combinations are thought to predominate depending on brain area, cell type and stage of neurodevelopment (Olsen and Sieghart, 2009). Relative spatial segregation of receptor subtypes is observed in ultrastructural and light microscopy studies, and in studies of phasic and tonic inhibition. Using subunit knock-in/-out mice and pharmacological tools, α1β2/3γ2 and α2β2/3γ2 receptors are localised to inhibitory synapses (Kasugai et al., 2010) where they mediate phasic inhibition, e.g. in hippocampal CA1 pyramidal neurons (Prenosil et al., 2006). By contrast, α5β3γ2, α4β3δ, α1βδ and α1β receptor isoforms mediate tonic inhibition in pyramidal and granule cells (Glykys et al., 2008; Stell et al., 2003; Sun et al., 2004; Glykys et al., 2007; Mortensen and Smart, 2006; Zheleznova et al., 2008; Brickley and Mody, 2012; Thomas et al., 2005).

Although they can be spatially discrete, $GABA_A$Rs are highly dynamic and diffuse laterally within the neuronal plasma membrane between synaptic and extrasynaptic areas (Thomas et al., 2005; Bogdanov et al., 2006; Bannai et al., 2009). $GABA_A$Rs are inserted into the plasma membrane at extrasynaptic locations and synaptic receptors access inhibitory postsynaptic

microdomains by lateral diffusion. At such specialisations, $GABA_ARs$ are likely to be anchored by scaffold proteins such as gephyrin (Lorenz-Guertin and Jacob, 2018; Tyagarajan and Fritschy, 2014; Mukherjee et al., 2011) and GARLH-family proteins (Yamasaki et al., 2017) resulting in longer residences for synaptic receptors at inhibitory synapses. Nevertheless, the relative extent of synaptic and extrasynaptic receptor access to the inhibitory synapse, and the mechanisms that selectively prevent accumulation of extrasynaptic receptors at the synapse, are unknown. Presently, we know that α5 subunit-containing receptors interact with the extrasynaptic anchoring protein radixin (Hausrat et al., 2015) and this can retain these receptors at perisynaptic/ extrasynaptic locations. However, what restricts other $GABA_AR$ subtypes to extrasynaptic membrane domains is unknown.

To address this issue, we incorporated an α-bungarotoxin binding site (BBS) mimotope in the N-terminal extracellular domain of prominent hippocampal synaptic (α1 and α2) and extrasynaptic (α4, α5, and δ) subunits. This tag systematically allows the lateral diffusion of $GABA_ARs$ in proximity to gephyrin-containing inhibitory synapses to be resolved using single particle tracking with a uniform labelling strategy that is not dependent upon N-terminal receptor subunit-specific antibodies. Our results provide evidence that $GABA_AR$ subunit composition, as well as specific subunit intracellular motifs play critical roles in determining the localization of $GABA_ARs$ on neuronal surface membranes.

2. Materials and methods

2.1 cDNA and constructs

Wild-type α1, α2, α4, α5, δ, γ2L, β2 and β3 in pRK5 vector and eGFP in pEGFP-N1 vector, along with myc-tagged α5 and BBS-tagged α1 have been described previously (Hannan et al., 2015; Hannan and Smart, 2018; Loebrich et al., 2006). Gephyrin-GFP cDNA was provided by J. Kittler (UCL, UK). 13 amino acids encoding for the BBS site were cloned into the N-terminus of α2, α4, $\alpha5^{myc}$ and δ $GABA_AR$ subunits using PCR (Table 1) followed by ligation and transformation into competent bacteria and screening. A chimera of δ subunit where the intracellular loop 2 was exchanged with the equivalent loop of γ2L subunit ($\delta^{BBS\text{-}\gamma2loop}$) was created using restriction free cloning (Van Den Ent and Löwe, 2006). Briefly, a megaprimer of the γ2L loop was created by amplification using PCR (Table 1) followed by a second PCR with the megaprimer using δ^{BBS} as template. The fidelity of all cDNA constructs was validated using DNA sequencing.

Table 1 – Oligonucleotide sequences used for cloning BBS (5'-3')

Construct	Forward Primer	Reverse Primer
$\alpha2^{BBS}$	GTTTAGAACCATATCCAGATGAGGC TAAAAATAACATCACCATCTTT	TACTTTCATAATATCTCCAATCTTCTT GGATGTTAGCCAGCACCAAC
$\alpha4^{BBS}$	GTTTAGAACCATATCCAGATGAGAA ATTGTGCCCGGAAAATTTTACC	TACTTTCATAATATCTCCAGTCCTTTG AGTTCTGTCCTGGGGATTC
$\alpha5^{BBS}$	GTTTAGAACCATATCCAGATATCTTT TCGCAAATGCCAACTAGTT	TACTTTCATAATATCTCCATAGGTCCT CTTCGCTTATTAGCTTTTGTTCATCGT
δ^{BBS}	GTTTAGAACCATATCCAGATGACTA CGTGGGCTCCAACCTGGAGA	TACTTTCATAATATCTCCACCCAATGT CATTCATTGCTCTGGCGCCATG
$\delta^{BBS\text{-}\gamma2loop}$	CCCTGGTGGAGTATGCATTTGCCCA TTATTTTGTCAGCAACCGGAA	CCGGGAAGACGGCGCGGGCATAGG AGTCCATTTTGGCAATGCGAAT

2.2 Cell culture and transfection

HEK-293 cells were grown at 37°C and 95% air /5% CO_2 in Dulbecco's modified Eagle's medium containing 10% (v/v) fetal calf serum (FCS), penicillin-G/ streptomycin (100 U/ ml and 100 µg/ ml) and 2 mM L-glutamine. For imaging and electrophysiology, cells were seeded onto 22 mm glass coverslips (VWR), coated with poly-L-lysine (Sigma). All media reagents were acquired from ThermoFisher unless otherwise stated.

For electrophysiology, HEK-293 cells were transfected with equimolar cDNAs of α, β2 or β3 and δ or γ2L $GABA_AR$ subunits along with eGFP using a calcium phosphate method (Hannan et al., 2011) 1-2 hr after plating. For imaging experiments equimolar cDNAs of wild-type or BBS-tagged cDNAs and eGFP were transfected.

Primary rat hippocampal cultures were prepared from E18 Sprague-Dawley embryos as described previously (Hannan et al., 2011). Dissected hippocampi were dissociated into single cells and seeded onto poly-D-lysine (Sigma) coated glass coverslips in a plating medium consisting of minimum essential media supplemented with 5% v/v heat-inactivated FCS, 5% v/v heat-inactivated horse serum, penicillin-G/ streptomycin (100 U/ 100 µg/ml), 2 mM L-glutamine, and 20 mM glucose (Sigma). Neurons were grown at 37°C and 95% air /5% CO_2. 2 hr after seeding the plating media was replaced with serum free maintenance media: Neurobasal-A supplemented with 1% v/v B-27, penicillin-G/ streptomycin (100 U /100 µg/ml), 0.5% v/v Glutamax and 35 mM glucose.

Neurons were transfected at 7 days *in vitro* (*DIV*) using a calcium phosphate based method (Hannan et al., 2013) using equimolar cDNAs of wild-type or BBS-tagged cDNAs and eGFP or gephyrin-GFP.

All tissue collection for neuronal cultures was undertaken in accordance with the Animals (Scientific Procedures) Act, 1986.

2.3 Antibody labelling and confocal imaging

Approximately 36 – 48 hr after transfection, HEK-293 cells expressing wild-type or BBS-tagged cDNAs were washed with phosphate buffered saline (PBS), fixed in 4% paraformaldehyde for 10 min at room temperature (RT) followed by permeabilisation in 0.1% Triton X-100 for 10 min and incubation in 400 nM α-BgTx-Alexa Fluor 555 (AF555) for 10 min. Cells were imaged

immediately after fluorescence labelling using a Zeiss LSM 510 confocal microscope equipped with an Achroplan x40 (NA 0.8) water objective as described previously (Hannan et al., 2013). Optimal z-sections of identified cells were imaged as a mean of 2 scans in 16 bit using a 543 nm Helium-Neon laser and a 560 nm long-pass filter for α-BgTx-AF555 and a 488 Argon laser with 505-530 nm band-pass filter for eGFP.

2.4 Whole cell patch clamp electrophysiology

GABA-activated whole cell currents were recorded 36 – 48 hr after transfection from HEK-293 cells expressing wild-type or BBS-tagged heteromers. Cells were superfused with a Krebs saline solution containing (mM): 140 NaCl, 4.7 KCl, 2.52 $CaCl_2$, 1.2 $MgCl_2$, 11 glucose, and 5 HEPES; pH 7.4. Borosilicate glass patch electrodes (3-5 MΩ) were filled with an internal solution containing (mM): 120 CsCl, 30 KOH, 11 EGTA, 10 HEPES, 2 K_2ATP, 1 $CaCl_2$, and 1 $MgCl_2$; pH 7.2. Membrane currents were filtered at 5 kHz (-3 dB, 6th pole Bessel, 36 dB/ octave) and cells were voltage clamped at a holding potential of -20 to -40 mV with optimised series resistance (Rs, <10 MΩ) and whole-cell membrane capacitance compensation.

Concentration-response curves were generated by measuring the current (I) for each GABA concentration and normalising the current to the maximal GABA response (I_{max}). Data were fitted using the Hill equation:

$$I / I_{max} = (1 / (1 + (EC_{50} / [A])^n)$$

where A is the concentration of GABA, EC_{50} is the concentration of GABA giving 50% of the maximum response and n is the Hill slope.

2.5 Imaging quantum dot-tagged $GABA_ARs$

Hippocampal neurons were labelled with quantum dots (QDs) at 12-14 DIV by incubating with 200-400 nM biotinylated α-BgTx (BgTx-B) for 2 min at 37 °C followed by washes in Krebs solution (3x) and incubation in 50 pM QD 655 conjugated to streptavidin in QD binding buffer (containing 2% w/v bovine serum albumin, 1 mM sodium azide, 215 mM sucrose) for 1 min at 37°C, as described previously (Hannan et al., 2016). After thorough washes, the coverslips were loaded in a temperature controlled (37°C) chamber (Solent Scientific) and imaged live within 5 min of mounting.

An Olympus IX71 wide-field inverted microscope with a 60X objective (NA – 1.35; Olympus), a halogen light source (PhotoFluor-II Metal Halide illumination system) and a back-illuminated iXon3 885 (Andor Technology) cooled electron-multiplying charge coupled device (EMCCD) camera was used to image $GABA_AR$-QD complexes for single particle tracking. A band-pass excitation filter (Semrock, 457 – 487 nm), a long-pass emission filter (496 nm), and dichroic mirror (495 nm) were used to image eGFP, and for imaging QD655, a 415 - 455 nm band-pass excitation filter, a 647.5 - 662.5 nm band-pass emission filter, and a 510 nm dichroic mirror were utilised.

For imaging QD specificity, single images with optimal exposure (30 - 150 ms) were captured in 16 bits using CairnMetamorph Meta Imaging software (Molecular Devices; version 7.7.10). Real-time movement of $GABA_AR$-QD complexes was captured by first selecting a region-of-interest (ROI) and taking an image of eGFP expression with typical exposure of ~30 - 150 ms, after which the filters were changed to image QDs in the same ROI and plane of view at 33 Hz for 300 frames.

2.6 Single particle tracking

Particle tracking of single $GABA_AR$-QDs (identified by their characteristic fluorescent 'blinking') was carried out as described previously (Hannan et al., 2016; Bannai et al., 2006). A custom Matlab (MathWorks) plugin, SPTrack (Ver5), was used to compile trajectories of QD movement. The centre of each QD was determined by a 2-D Gaussian fit with a spatial resolution of ~10 – 20 nm for every image taken consecutively in frame sequence. For a single QD, the centre of the Gaussian peak identified in successive image frames were track-connected, based on estimated diffusion coefficients and the likelihood of the two Gaussian peaks in consecutive frames belonging to the same QD track. QDs trajectories that contained less than 15 consecutive frames were discarded.

The mean square displacement (MSD) of each QD was calculated using the following equation:

$$\mathrm{MSD}\,(ndt) = (N - n)^{-1} \cdot \Sigma_{i=1}^{N-n} ((x_{i+n} - x_i)^2 + ((y_{i+n} - y_i)^2)$$

where x_i and y_i are the spatial co-ordinates of a single QD identified in a single image frame *i*. *N* is the total number of points in the QD trajectory, *dt* is the time interval between two successive frames (33 ms), and *ndt* is the time interval over which the mean square displacement is

averaged. From the MSD plot, the diffusion coefficient, *D*, for a QD was calculated by fitting the first two to five points of the MSD plot against time with the following expression:

$$\text{MSD}\ (t) = 4D_{2-5}\,t + 4\sigma_x^2$$

where σ_x is the QD localization accuracy in one dimension. D was determined from the slope of the relationship. Given the inherent noise in CCD imaging systems, and the errors in accurately locating single QDs as a result, those trajectories with $D < 10^{-4}$ μm^2 s^{-1} were considered immobile and excluded from calculations of the median D.

Synaptic terminals, identified by gephyrin-GFP puncta, were thresholded using ImageJ, and co-localised QD trajectories were defined as synaptic. QD data were subsequently analysed using Origin ver 6, Matlab, Graphpad Instat 3, and SPSS ver 25.

3. Results

3.1 Inserting the α-bungarotoxin binding site into GABA$_A$R isoforms

The membrane diffusion of synaptic and extrasynaptic GABA$_A$R subtypes was studied using a uniform labelling strategy that involved incorporating a mimotope for the α-bungarotoxin (α-BgTx) binding site (BBS) into the N-terminus of α1 (Hannan and Smart, 2018), α2, α4, α5 and δ GABA$_A$-R subunits (Fig. 1A). Since α-BgTx is a low affinity, low efficacy antagonist of GABA$_A$Rs (Hannan et al., 2015), we applied low (sub-inhibitory) concentrations of 400 nM and tested the specificity of our labelling strategy in heterologous expression systems. α-BgTx coupled to Alexa Fluor 555 (α-BgTx-AF555) bound to cells expressing BBS-tagged receptors in permeabilised HEK-293 cells without labelling either wild-type subunits or just eGFP expressing controls (Fig. 1B) suggesting that recombinant N-terminal located BBS sites can be used to label specific GABA$_A$R subunits.

To verify that the insertion of the BBS tag did not affect signalling via epitope-tagged GABA$_A$Rs composed of either αβγ or αβδ subunits, we constructed concentration response curves to GABA. Similar to previous results using α1^{BBS} receptors (Hannan and Smart, 2018), the potency of GABA showed only minor changes (2-3-fold) due to the presence of the BBS tags (Fig 1C-D).

Together these results suggest that the BBS can be used for specific labelling of GABA$_A$R subunits acting as a functionally-silent site for imaging receptor trafficking.

3.2 Specificity of Quantum Dot labelling in neurons via the α-bungarotoxin binding site

Given the low affinity of α-BgTx binding to GABA$_A$R heteromers previously reported to occur at the GABA orthosteric binding site interface (Hannan et al., 2015), we deduced that application of low concentrations α-BgTx will bind readily to the higher affinity (Harel et al., 2001; Hannan et al., 2011) BBS epitope avoiding significant inhibition caused by occupancy of the endogenous interfacial subunit site. Recombinant GABA$_A$Rs were labelled with quantum dots (QDs) after expression in cultured hippocampal neurons using low 200 – 400 nM concentrations of α-BgTx-biotin (BgTx-B) and 50 pM QD655 streptavidin. Neurons were transfected with single GABA$_A$R subunit constructs along with eGFP at 7 days *in vitro* (*DIV*) and imaged at 12-14 *DIV*. Under these conditions, specific labelling with QDs was observed when BBS-tagged GABA$_A$R subunits were expressed. Labelling with QDs was negligible when untagged GABA$_A$R subunits or just

eGFP were expressed (Fig 2A). Moreover, no labelling was observed when BBS-tagged receptors were incubated in unlabelled α-BgTx along with QD655 further validating the specificity of our labelling (Fig 2A).

Finally, to validate the sensitivity of our labelling strategy for tagging $GABA_ARs$ with QDs, we performed proof-of-principle experiments by studying the lateral diffusion of α1-subunit containing $GABA_ARs$ (α1-$GABA_ARs$) in response to the microtubule destabilizer nocadazole (10 μM for 1 hr at 37°C). Nocodazole treatment will de-cluster $GABA_ARs$ (Petrini et al., 2004) and it increases the lateral mobility of other Cys-loop receptors, e.g., nicotinic acetylcholine receptors (Fernandes et al., 2010; Burli et al., 2010). The lateral diffusion of synaptic and extrasynaptic α1-$GABA_ARs$ was studied in hippocampal neurons using single particle tracking of QDs after expression of single BBS-tagged subunits together with the inhibitory postsynaptic density marker, gephyrin-GFP (Muir et al., 2010). In accord with previous reports (Gouzer et al., 2014; Gerrow and Triller, 2014), α-BgTx labelling revealed that α1-$GABA_ARs$ were recruited to inhibitory synapses following lateral diffusion (Fig 2B), and that synaptic receptors diffuse more slowly compared to their extrasynaptic counterparts (Fig 2C-D, $P<0.05$, Mann-Whitney U (MWU) test). As predicted, nocadazole increased the diffusion coefficients (D) for synaptic (median $D_{control}$ - 0.05 $\mu m^2 s^{-1}$, n = 87 receptors; $D_{nocadazole}$ - 0.06 $\mu m^2 s^{-1}$, n = 132, n = receptors, $P<0.01$, MWU test; Fig 2C-D) as well as for extrasynaptic receptors ($D_{control}$ - 0.07 $\mu m^2 s^{-1}$, n = 1741; $D_{nocadazole}$ - 0.08 $\mu m^2 s^{-1}$, n = 1852 receptors, $P<0.05$, MWU test; Fig 2C-D), indicative of increased lateral diffusion of α1-$GABA_ARs$ due to untethered movement.

These results suggest that the BBS site allows specific labelling of single $GABA_ARs$ in hippocampal neurons and can be applied to study lateral diffusion of different $GABA_AR$ subunits.

3.3 $GABA_AR$ subunits exhibit differential lateral mobility at inhibitory synapses

Having validated the BBS tagging approach for studying $GABA_AR$ lateral diffusion, we next compared the diffusion profiles of subunits considered to form key components of phasic (α2) and tonic (α4, α5 and δ) inhibition. As noted previously (Gouzer et al., 2014), α2-tagged $GABA_ARs$ were clearly segregated into three distinct populations defined as: synaptic, extrasynaptic and exchanging (Fig 3A). In comparison, α4, α5 and δ-containing receptors that typically mediate tonic inhibition, and are thus considered to reside in the extrasynaptic membrane, also accessed the synaptic membrane by lateral diffusion (Fig 3A). This profile has

been reported for α5 receptors (Gerrow and Triller, 2014; Renner et al., 2012), but not for α4 or δ receptors. The median diffusion coefficients for α2 at inhibitory synapses were lower compared to α4 and δ subunits (synaptic $D_{\alpha2}$ – 0.02 $\mu m^2 s^{-1}$, n = 221 receptors; $D_{\alpha4}$ – 0.028 $\mu m^2 s^{-1}$, n = 294 receptors; $D_{\alpha5}$ – 0.023 $\mu m^2 s^{-1}$, n = 248 receptors; D_{δ} – 0.025 $\mu m^2 s^{-1}$, n = 1002 receptors; Fig 3B-D, P<0.001 (δ), P<0.01 (α4), MWU test). This suggests that while resident, if only briefly, at inhibitory synapses $GABA_AR$ lateral diffusion is dependent on subunit composition.

Moreover, with regard to confinement at inhibitory synapses, δ-$GABA_A$Rs were least confined compared to α2, α4 and α5 receptors (median synaptic confinement area, CA_{δ} – 0.25 μm^2, $CA_{\alpha2}$ – 0.18 μm^2, P<0.001, MWU test; $CA_{\alpha4}$ – 0.23 μm^2, P<0.01, MWU test; $CA_{\alpha5}$ – 0.18 μm^2, P<0.001, MWU test Fig 3E-F). Interestingly, α4 receptors were also less confined compared to α2, and α5 receptors (P<0.05 and P<0.01 MWU test). This would accord with the classical extrasynaptic receptor subunits being retained less compared to their synaptic counterparts.

The dwell time for BBS-tagged $GABA_A$Rs at inhibitory synapses also varied with the subunits. Synaptic dwell times were notably higher for α2- and α4- compared to α5- and δ-$GABA_A$Rs (mean dwell time (*DT*), $DT_{\alpha2}$ – 3.9 ± 0.2 s, n = 257 receptors; $DT_{\alpha4}$ – 4.1 ± 0.2 s, n = 297 receptors; $DT_{\alpha5}$ – 3.2 ± 0.2 s, n = 329 receptors; DT_{δ} – 3.3 ± 0.1 s, n = 841 receptors; Fig 3G, P<0.05, P<0.01, P<0.001, One-way ANOVA). Consistent with this, the ratio of exchanging receptors (between postsynaptic and extrasynaptic domains) to total synaptic receptors (Renner et al., 2009) was higher for α5- (1.89, n = 478) and δ- (1.89, n =1657) compared to α2- (1.17, n = 320) and α4-$GABA_A$Rs (1.12, n = 461) reflecting reduced residence of α5- and δ- $GABA_A$Rs at synapses.

These results indicate that $GABA_A$Rs associated with phasic and tonic inhibition are both able to access inhibitory synaptic membranes by lateral diffusion, although subunits forming two major classes of extrasynaptic $GABA_A$Rs (α5 and δ) are not retained at inhibitory synapses to the same extent as α2- and α4-$GABA_A$Rs. The trend towards slower diffusion, coupled to a smaller confined area occupied by α5-$GABA_A$Rs compared to δ-counterparts, may reflect the accumulation of α5-containing receptors at perisynaptic, radixin-containing domains where α5-$GABA_A$R activity will slow the kinetics of IPSCs (Zarnowska et al., 2009; Hausrat et al., 2015).

3.4 $GABA_AR$ subunits exhibit differential lateral mobility in the extrasynaptic membrane

Analysis of the membrane diffusion profiles for extrasynaptic $GABA_A$Rs revealed that δ-$GABA_A$Rs were the slowest to traverse the membrane, surprisingly α5-$GABA_A$Rs were fastest, and α2- and α4-$GABA_A$Rs were ranked intermediate (extrasynaptic $D_{α2}$ – 0.043 $μm^2s^{-1}$, n = 8435 receptors; $D_{α4}$ - 0.045 $μm^2s^{-1}$, n = 6623 receptors; $D_{α5}$ – 0.058 $μm^2s^{-1}$, n = 7917 receptors; $D_{δ}$ – 0.037 $μm^2s^{-1}$, n = 30132 receptors; Fig 4A-C, P<0.05 and P<0.001, MWU test). The lower diffusion coefficients noted for extrasynaptic δ-$GABA_A$Rs suggested that their mobility must be limited by diffusional constraints. In extrasynaptic membrane areas, α2 receptors were most confined followed by δ, α4 and α5 (median extrasynaptic confinement area, $CA_{α2}$ – 0.25 $μm^2$, $CA_{α4}$ – 0.29 $μm^2$, $CA_{α5}$ – 0.30 $μm^2$, $CA_{δ}$ – 0.28 $μm^2$, Fig 4D-E, P<0.05 and P<0.001, MWU test)

These results suggest that while α5 receptors diffuse more freely in the extrasynaptic membrane domains, δ and α2 receptors have, by contrast, restrained diffusion, which may reflect associations with receptor-associated molecules. Such results are in accord with δ-$GABA_A$Rs being retained at extrasynaptic locations, though unexpectedly, this could also apply to α2-$GABA_A$Rs, which could contribute to tonic inhibition by their extrasynaptic location (Durkin et al., 2018).

3.5 Dependence of extrasynaptic $GABA_AR$ lateral mobility on subunit structural domains

Given the reduced basal lateral diffusion of δ-$GABA_A$Rs in the extrasynaptic domain reflected by a smaller membrane confinement area and lower diffusion coefficient compared to other prominent extrasynaptic receptor subtypes (α4 and α5, Fig. 4), we investigated whether specific motifs played a role in confining δ-$GABA_A$Rs outside inhibitory synapses. The M4 domain of γ2 subunits play a critical role in clustering $GABA_A$Rs at synapses (Alldred et al., 2005), however, given the significant sequence homology (~78%) between the M4 domains for γ2 and δ subunits, we studied the large intracellular loop 2 (ICL2) where the sequence conservation falls to ~45% between γ2L and δ subunits. To do so, we created a δ subunit chimera in which ICL2 of this subunit was replaced with the equivalent ICL2 from γ2L subunits ($δ^{γ2loop}$; Fig 5A). The lateral diffusion of the chimeric receptor was then assessed. For wild-type δ-$GABA_A$Rs expressed in neurons, the cumulative probability distributions for extrasynaptic δ-receptor diffusion intersected the equivalent distribution for the δ-synaptic receptors at ~0.02 $μm^2s^{-1}$. This

suggested that a large fraction (~30%) of δ-GABA$_A$Rs in the extrasynaptic domain move more slowly than synaptic receptors (Fig 5B). Interestingly, for the δ$^{\gamma 2loop}$ chimera this intercept in the cumulative probability distributions was not observed between synaptic and extrasynaptic receptors as synaptic δ$^{\gamma 2loop}$ receptors were consistently slower (Fig 5B).

Incorporating the γ2L ICL2 into δ subunits increased diffusion for synaptic (D_δ – 0.029 μm^{2}s^{-1}, n = 226 receptors; $D_{\delta\text{-}\gamma 2loop}$ – 0.034 μm^{2}s^{-1}, n = 252 receptors; P<0.001, MWU test), as well as extrasynaptic δ-γ2 loop receptors (D_δ – 0.038 μm^{2}s^{-1}, n = 11868 receptors; $D_{\delta\text{-}\gamma 2loop}$ – 0.046 μm^{2}s^{-1}, n = 7457 receptors Fig 5B-C; P<0.05 MWU test).

In accord with increased diffusion, both synaptic and extrasynaptic membrane confinement areas for the chimeric δ$^{\gamma 2loop}$ receptor were increased compared to that for δ-GABA$_A$Rs (median synaptic CA_δ– 0.25 μm^2; $CA_{\delta\text{-}\gamma 2loop}$ – 0.27 μm^2*;* median extrasynaptic CA_δ– 0.28 μm^2; $CA_{\delta\text{-}\gamma 2loop}$ – 0.30 μm^2; Fig 5D-F; P<0.001; KS test; P<0.05 and P<0.001, MWU test). The importance of the γ2L loop for regulating the mobility profile of δ-GABA$_A$Rs was evident from the synaptic trapping of these receptors. Inserting the γ2L loop into δ-GABA$_A$Rs increased the synaptic dwell times over their δ-subunit counterparts by ~24 % (DT_δ - 3.3 ± 0.2, n = 259; $DT_{\delta/\gamma 2loop}$ – 4.1 ± 0.2, n = 297; Fig 5G; P<0.05, two-tailed unpaired t-test).

These results indicate that the ICL2 of γ2L subunits increased the trapping of GABA$_A$Rs at inhibitory synapses. Moreover, the movement of δ subunits are controlled by diffusional constraints in the extrasynaptic membrane domain compared to other GABA$_A$R subunits that have been studied in this investigation, and previously (Renner et al., 2012). The ICL2 of the δ subunit is important for reducing their lateral mobility and causing confinement to smaller areas of the extrasynaptic membrane.

3.6 Agonist-induced lateral mobility characteristics of GABA$_A$Rs

Although subunit identity clearly can affect GABA$_A$R diffusion and mobility it is less clear whether the activation state of the receptor also influences mobility. Prolonged activation of neurotransmitter receptors can lead to excessive signalling and desensitisation. Previous reports indicate that chronically-activated receptors are often removed from synapses and the entry of new receptors restricted (Borgdorff and Choquet, 2002; Groc et al., 2004; Mikasova et al., 2008).

To determine if the state of receptor activation also modulates receptor diffusion, we investigated the effect of the potent GABA agonist muscimol on the lateral mobility of synaptic (α2) and extrasynaptic receptor (α4) subtypes. Acute application of 100 μM muscimol did not alter the lateral diffusion of either α2- or α4-$GABA_A$Rs at inhibitory synapses ($D_{α2\text{-control}}$ – 0.02 $μm^2s^{-1}$, n = 188 receptors; $D_{α2\text{-muscimol}}$ – 0.014 $μm^2s^{-1}$, n = 131 receptors; $D_{α4\text{-control}}$ – 0.022 $μm^2s^{-1}$, n = 214 receptors; $D_{α4\text{-muscimol}}$ – 0.024 $μm^2s^{-1}$, n = 178 receptors; Fig 6A-C, P>0.05, MWU test). Furthermore, the synaptic confinement area for each receptor subtype at gephyrin-positive inhibitory synapses was also unaffected (median $CA_{α2\text{-control}}$ – 0.16 $μm^2$; $CA_{α2\text{-muscimol}}$ – 0.15 $μm^2$; $CA_{α4\text{-control}}$ – 0.2 $μm^2$; $CA_{α4\text{-muscimol}}$ – 0.2 $μm^2$; Fig 6D-E, P>0.05, MWU test). Similarly, the synaptic dwell times of α2 and α4 receptors (data not shown) were unaffected by muscimol.

By contrast, in extrasynaptic areas, both α2- and α4-$GABA_A$Rs showed differential mobilities. While lateral diffusion for α2-$GABA_A$Rs was reduced ($D_{α2\text{-control}}$ – 0.04 $μm^2s^{-1}$, n = 7599 receptors; $D_{α2\text{-muscimol}}$ – 0.03 $μm^2s^{-1}$, n = 4396 receptors; Fig 6F-H, P<0.001, MWU test), that for α4-$GABA_A$Rs was increased ($D_{α4\text{-control}}$ – 0.037 $μm^2s^{-1}$, n=4583 receptors; $D_{α4\text{-muscimol}}$ – 0.043 $μm^2 s^{-1}$, n = 3355 receptors; Fig 6F-H, P<0.01, MWU test) following receptor activation by muscimol. In parallel, the confinement area for α2-$GABA_A$Rs was reduced (median $CA_{α2\text{-control}}$ – 0.24 $μm^2$; $CA_{α2\text{-muscimol}}$ – 0.22 $μm^2$; Fig 6I-J, P<0.001, MWU test) whereas for α4-$GABA_A$Rs the membrane area increased ($CA_{α4\text{-control}}$ – 0.27 $μm^2$; $CA_{α4\text{-muscimol}}$ – 0.29 $μm^2$; Fig 6I-J, P<0.001, MWU test).

These results suggest that muscimol activation of $GABA_A$R subtypes can differentially modulate the kinetics of lateral diffusion for extrasynaptic receptors.

4. Discussion

The activation of neurotransmitter receptors at synapses is an important determinant of synaptic strength. Equally important are the mechanisms that govern the differential localisation and clustering of receptors since these will determine the cell surface numbers that can be activated by neurotransmitters. For $GABA_A$Rs, it has become increasingly clear that receptor mobility and the accessibility of anchoring molecules can impact on, and help to tune, GABAergic inhibition (Renner et al., 2012; Gouzer et al., 2014; Bannai et al., 2009; Mukherjee et al., 2011). Furthermore, desensitised $GABA_A$Rs can traverse between adjacent synapses by lateral diffusion (de Luca et al., 2017) thereby conferring from one inhibitory synapse to another, a receptor activation status that influences GABAergic inhibition. This diffusion is limited by glutamatergic activity and will therefore play a role in synaptic plasticity. In the present study, we have extended our α-BgTx labelling strategy, using minimalist tags as previously deployed for the study of $GABA_B$ receptors (Hannan et al., 2016), to explore the lateral diffusion of $GABA_A$R subunits, which are closely associated with synaptic and tonic inhibition.

The method we use reveals clear labelling of BBS-containing $GABA_A$Rs, but not of wild-type receptors lacking the inserted BBS. This indicates that the presence of the high-affinity BBS mimotope (Harel et al., 2001; Hannan et al., 2013) is required for labelling of $GABA_A$Rs by α-BgTx. Furthermore, at the concentrations of α-BgTx that were applied, we did not observe labelling of the inhibitory interfacial α-BgTx site we previously reported on wild-type receptors (Hannan et al., 2015), nor was there any inhibition of GABA currents evident, from using α-BgTx at 200 - 400 nM, which is below the inhibitory threshold of 5 – 10 μM. This suggests our labelling strategy was quite specific for the introduced BBS that had been inserted near the start of the extracellular domain, leaving $GABA_A$Rs functionally unaffected.

Moreover, QD labelling of $GABA_A$Rs was only evident in transfected hippocampal neurons when BBS-tagged subunits were expressed. Neurons expressing native subunits remained unlabelled, validating the use of low concentrations of α-BgTx that avoids affecting receptor function via the apparent low-affinity endogenous binding site on $GABA_A$Rs (Hannan et al., 2015). It is also unlikely that the expression of receptor subunits in neurons will affect the equilibrium of cell surface receptors (e.g. by over-expression) since the BBS-tagged $GABA_A$R α2, α4, α5 and δ subunits will require co-assembly with endogenous subunits to form receptor pentamers. Thus, collectively, the smaller size of the α-BgTx molecule compared to an antibody

(Hannan et al., 2013) coupled to the functional neutrality of the inserted BBS makes this receptor tagging method an attractive tool for probing the lateral diffusion of $GABA_A$Rs.

Our results demonstrate that $GABA_A$Rs dynamically diffuse along neuronal membranes including inhibitory postsynaptic membranes, and also extrasynaptic membrane domains, with receptors transferring between the two compartments by lateral diffusion. The α2, α4, α5 and δ receptors tagged in this study accessed all membrane domains, an observation which did not initially appear to be in accord with their presumed roles in synaptic and tonic inhibition. Imaging studies suggest that in the dentate gyrus of the hippocampus, synaptic $GABA_A$Rs are most likely composed of α1 or α2βγ receptors (Nusser et al., 1996) with α4β and δ-containing receptors forming the predominant extrasynaptic receptor populations (Sun et al., 2004; Chandra et al., 2006); by contrast α5βγ $GABA_A$Rs predominate as extrasynaptic receptors in CA1 pyramidal cells (Caraiscos et al., 2004; Glykys et al., 2008).

Given the ability of α2, α4, α5 and δ to traverse all membrane areas, it seems probable that there is no clear membrane demarcation area between $GABA_A$Rs containing specific subunits supporting phasic and tonic inhibition. It is notable that whilst $GABA_A$Rs underpinning both phasic and tonic inhibition travel to and from the inhibitory synapse, what prevents typically extrasynaptic receptors (e.g., δ subunit-containing) from mediating phasic inhibition while they are at the synapse is unclear. This traditional view needs to be reinterpreted given our evidence here and that from using a picrotoxin-insensitive reporter mutation in δ subunits (Sun et al., 2018). It is clear that pharmacologically-tagged δ subunits can contribute to the inhibitory postsynaptic current (IPSC; Sun et al., 2018). By comparison, it is quite plausible for classical synaptic $GABA_A$Rs, when present in the extrasynaptic domain (Bogdanov et al., 2006; Thomas et al., 2005), to support tonic inhibition, even though some receptors will have different sensitivities to GABA with γ2 subunit-containing receptors being less sensitive compared to δ subunit-containing counterparts.

The presence of γ2-$GABA_A$Rs in the extrasynaptic domain reflects the mechanisms involved in replenishing surface receptors following internalisation and delivery of *de novo* synthesized or recycled phasic receptor subunits via endo-/ exocytosis at extrasynaptic membranes (Bogdanov et al., 2006; Thomas et al., 2005; Moss and Smart, 2001; Lorenz-Guertin and Jacob, 2018; Luscher et al., 2011) membranes. From these sites, close to inhibitory synapses, they can diffuse into inhibitory synapses (Bogdanov et al., 2006; Thomas et al., 2005). The concept of receptors being subject to confinement in a membrane subdomain (Choquet and Triller, 2013)

could explain why extrasynaptic receptors, have limited entry into synapses because of membrane diffusion restraints and/or interactions with extrasynaptic anchoring molecules, e.g. radixin (Hausrat et al., 2015).

By studying the diffusion coefficients for subunits at inhibitory synapses, it was noticeable that the mobility of α2 were relatively reduced compared to α4- and δ-$GABA_A$Rs. This disparity suggests that most α2 subunits at synapses are likely to be devoid of δ subunits and possibly associate with γ subunits compared to α4- and δ-subunits that can co-assemble (Olsen and Sieghart, 2009). In addition, α5 subunits mediate a key component of tonic inhibition in the hippocampus and these receptors can be perisynaptically localised to gephyrin synapses (Hausrat et al., 2015; Brady and Jacob, 2015; Serwanski et al., 2006). Indeed γ-containing α2 and α5 receptors are important for generating fast and slow IPSCs, respectively, in hippocampal pyramidal neurons (Essrich et al., 1998; Zarnowska et al., 2009). The differences in synaptic membrane confinement areas for α2/ α5 and δ also support the concept that α2 and α5 co-assemble with γ2 subunits, since the former are more confined at synapses compared to δ subunits.

Interestingly, the diffusion coefficients for α4 and δ receptors were similar at synapses although a decrease in membrane confinement area and longer synaptic dwell times for α4 subunits compared to δ may suggest that at least some α4 subunits will not contain δ subunits, which likely reflects assembly with γ2 subunits. Consistent with their previously ascribed roles in mediating tonic inhibition, synaptic dwell times for δ subunits are lower compared to α2 and α4 subunits but similar to α5. Further comparison reveals that α5-$GABA_A$Rs also have a tendency towards smaller confinement areas at synapses compared to δ and α4 but similar to α2, suggesting their movement may be restricted around inhibitory synapses, potentially reflecting interactions with other proteins (e.g. radixin). Interestingly α4 receptors had higher dwell times than for δ subunits at synapses suggesting the existence of non δ-containing α4 heteromers which may reside in or near inhibitory synapses. Indeed, α4β receptors have been previously proposed (Sieghart and Sperk, 2002) but whether they participate in synaptic inhibition is unclear. Moreover, heteromeric receptors in which two different α subunits can exist in the same pentamer may also explain mixed cell surface mobility profiles and behaviour (McKernan et al., 1991).

For the extrasynaptic receptors that contain α5 subunits interactions with radixin (Hausrat et al., 2015) retain such $GABA_A$Rs outside inhibitory synapses. However, no interacting partners able to secure exclusion from the synaptic membrane have thus far been discovered for other extrasynaptic receptors such as δ. Our analyses suggest that δ- and α2-receptors likely experience similar diffusional constraints in the extrasynaptic membrane, since their diffusion coefficients were both lower compared to those for α4 and α5-receptors. This could reflect co-assembly of α2 with δ subunits to form α2βδ receptors. Notably, the membrane area in which α2 subunits are confined is also smaller compared to those for α4 and α5-receptors. By comparison with α2, α4 and δ subunits, α5-$GABA_A$Rs in the extrasynaptic domain showed the highest diffusion coefficient implying increased mobility of α5-receptors possibly released from radixin binding and prior to clustering at perisynaptic sites outside inhibitory synapses.

Another interesting observation from studying extrasynaptic receptors is that α2-$GABA_A$Rs diffuse slower and in a more confined area than α4 and α5 receptors. These α2 subunits could feasibly be populating inhibitory synapses that are not always co-habited by gephyrin. For example, recently identified markers of inhibitory synapses such as LHFPL4/ GARLH (Davenport et al., 2017; Yamasaki et al., 2017) and InSyn1/2 (Uezu et al., 2016) suggest other inhibitory synaptic markers are likely to be important particularly as ablating gephyrin in neurons only reveals a small reduction in IPSC amplitudes but not frequency (Levi, 2004).

To understand further why δ-$GABA_A$Rs underpin tonic inhibition and apparently stay in the extrasynaptic domain, we generated chimeric constructs switching the intracellular loop 2 region of δ for the γ2L equivalent. The underlying hypothesis on which this was based assumed that extrasynaptic δ receptors were subject to high diffusion constraints because they were anchored outside inhibitory synapses via unique motifs on this subunit. Interestingly, the intracellular loop 2 of δ subunits is important in this regard, since its replacement by the equivalent loop of γ2L largely relieved the diffusional constraints, increasing receptor diffusion and its membrane area of confinement in the extrasynaptic domain. Furthermore, the dominance of the γ2L loop 2 in the δ subunit also resulted in increased synaptic dwell times, presumably because the receptor behaves more akin to an αβγ isoform than αβδ. Overall, these results strongly suggest that δ-receptors are diffusion restricted because of subunit interactions with unknown partners via the large intracellular loop 2 region.

Aside from structural motifs and subunit identity influencing the lateral mobility of cell surface $GABA_A$Rs, the state of receptor activation is also important (Gouzer et al., 2014). Our brief

exposure of α2- and α4-receptors to the potent, selective $GABA_AR$ agonist, muscimol, revealed no effect on the lateral diffusion of these receptors at inhibitory synapses. This is contrary to a previous report (Gouzer et al., 2014) in which increased diffusion of synaptic α2-receptors was observed with muscimol. However, the concentration-time profiles between the studies are quite different ranging from high concentration, brief exposure (100 μM, 5 min) to low concentration, prolonged exposure (10 μM, 30 min). Such differences may reflect differential entry and sojourns into one or more desensitised states that could affect receptor mobility or differences between labelling strategies (antibody vs α-BgTx labelling) and reaffirm the view that activation state is an important determinant of receptor mobility. Neither study reported any change in receptor dwell times upon activation at inhibitory synapses and therefore no change of α2-receptor trapping at the synapse. However, for extrasynaptic α2- and α4-$GABA_ARs$, agonist activation reduced the mobility of α2- and increased that for α4-receptors with concomitant reduction (α2-) and increase (α4-$GABA_AR$) in the membrane areas of confinement. At the concentration of muscimol used (100 μM), all $GABA_ARs$ will be desensitised (Mortensen et al., 2010) and presumably increased confinement to extrasynaptic domains with reduced diffusion will limit the replenishment of synaptic $GABA_ARs$. Under similar conditions, increased extrasynaptic diffusion for α4-receptors may form part of the process that facilitates agonist-induced internalisation (Connolly et al., 1999; Kittler et al., 2000). Thus for both α2- and α4-receptors signalling will be restricted not just functionally but also numerically under desensitising conditions. What happens in the presence of $GABA_AR$ antagonists is also informative as in this regard as these receptors are constantly activated at postsynaptic densities due to presynaptic GABA release and some isoforms show spontaneous activity even at extrasynaptic locations (Wlodarczyk et al., 2013). Increases of synaptic dwell times in the presence of receptor antagonists (Gouzer et al., 2014) suggest the reverse interplay whereby the availability of synaptic receptors are increased under closed/ antagonised states.

Together our results suggest that $GABA_ARs$ are under variable diffusional constraints at synaptic and extrasynaptic areas and subunit identity and subunit domains will significantly determine their lateral diffusion properties.

Acknowledgments

This work was supported by the MRC and Wellcome Trust

Figure legends

Fig 1. Cloning α-bungarotoxin binding sites on $GABA_ARs$

A, Schematic and primary amino acid sequences showing sites of insertion of α-bungarotoxin (α-BgTx) binding sites (BBS) in α1, α2, α4, α5 and δ subunits. *B,* Confocal images showing labelling of $GABA_ARs$ in permeabilised HEK-293 cells with α-BgTx Alexa Fluor 555 (AF555). Note only subunits with the BBS tag were bound to α-BgTx AF555. Scale bar = 10 μm. *C,* GABA-activated currents from wild-type and BBS-tagged $GABA_ARs$. *D,* GABA-activated concentration response curves for wild-type and BBS-tagged $GABA_ARs$. EC_{50}s: α1β2γ2L – 6.7 ± 0.1 μM, n = 7; $α1^{BBS}$β2γ2L – 18.7 ± 0.5 μM, n = 10; α2β2γ2L – 17.5 ± 2.2 μM, n = 7; $α2^{BBS}$β2γ2L – 59.4 ± 4.8 μM, n = 10; α4β2γ2L – 5.3 ± 0.2 μM, n = 7; $α4^{BBS}$β2γ2L – 4.8 ± 0.5 μM, n = 7; α5β2γ2L – 5.7 ± 0.25 μM, n = 7; $α5^{BBS}$β2γ2L – 3.6 ± 0.1 μM, n = 6; α4β3δ - 2.03 ± 0.3 μM, n = 6; $α4β3δ^{BBS}$ - 1.1 ± 0.02μM, n = 6. Points are mean ± SEM.

Fig 2. Validation of $GABA_AR$ QD labelling

A, Images of QD labelling specificity of BBS-tagged α1, α2, α4, α5 and δ subunits. Note that labelling was only present for neurons expressing $α1^{BBS}$, $α2^{BBS}$, $α4^{BBS}$, $α5^{BBS}$ or $δ^{BBS}$ subunits. No labelling occurs for neurons expressing wild-type α1, α2, α4, α5 and δ subunits or when cells expressing BBS-tagged α4-$GABA_ARs$ were incubated in biotin-linked BgTx (BgTx-B), QDs or with unlabelled α-BgTx and QD (uBTX+QD). Scale bar = 5 μm. *B,* Example trajectories of synaptic, extrasynaptic and exchanging QD-tagged α1-$GABA_ARs$ around gephyrin-eGFP expressing inhibitory synapses. The white signals represent QDs. Scale bar = 1 μm. *C,* Cumulative probability distributions of diffusion coefficients for synaptic and extrasynaptic α1-$GABA_ARs$ in control and +10 μM nocodazole (Noc). Inset, mean square displacement of synaptic and extrasynaptic α1-$GABA_ARs$ in control and +nocodazole. *D,* 25-75% interquartile range (IQR) and median diffusion coefficient of synaptic (Syn) and extrasynaptic (ESyn) α1-$GABA_ARs$ in control (C) and nocodazole (N). *P<0.05, **P<0.01, KS test, n = 87 – 1852.

Fig 3. Diffusion of synaptic $GABA_ARs$

A, Example trajectories of synaptic, extrasynaptic and exchanging QD-tagged α2, α4, α5 and δ $GABA_ARs$ around gephyrin-eGFP expressing inhibitory synapses. The white signals represent QDs. Scale bar = 1 μm. *B,* Cumulative probability distributions of diffusion coefficients (D) for synaptic $GABA_ARs$. *C,* Mean square displacement of synaptic $GABA_ARs$. *D,* 25-75% interquartile range (IQR) and median diffusion coefficient of synaptic $GABA_ARs$. *E,* Cumulative

probability distributions of confinement area for synaptic $GABA_A$Rs. *F,* 25-75% interquartile range (IQR) of median confinement area for synaptic $GABA_A$Rs. *G,* Synaptic dwell times for α2, α4, α5 and δ $GABA_A$Rs. *P<0.05, **P<0.01, ***P<0.01; KS test for *(D)* and *(F)*, One-way ANOVA for *(G)*. n = 221 – 1002.

Fig 4. Diffusion of extrasynaptic $GABA_A$Rs

A, Cumulative probability distributions of diffusion coefficients for extrasynaptic $GABA_A$Rs. *B,* Mean square displacement of extrasynaptic $GABA_A$Rs. *C,* 25-75% interquartile range (IQR) and median diffusion coefficient for extrasynaptic $GABA_A$Rs. *D,* Cumulative probability distributions of confinement area of extrasynaptic $GABA_A$Rs. *E,* 25-75% interquartile range (IQR) and median confinement area for extrasynaptic $GABA_A$Rs. **P<0.01, ***P<0.001, KS test, n = 6623 – 30132.

Fig 5. Extrasynaptic diffusion restraint on δ subunits relieved by γ2 intracellular domain

A, Schematic of a δ subunit chimera in which intracellular loop 2 is exchanged for its equivalent in γ2L (red). *B,* Cumulative probability distributions of synaptic and extrasynaptic diffusion coefficients of δ subunits and δ/γ2 loop chimera ($\delta^{\gamma2loop}$). Arrow shows cross-over point of synaptic and extrasynaptic cumulative probability distributions. *C,* 25-75% interquartile range (IQR) and median diffusion coefficients of synaptic (Syn) and extrasynaptic (ESyn) δ subunits and δ/γ2 loop chimera ($\delta^{\gamma2}$). *D,* Mean square displacement of synaptic and extrasynaptic δ subunits and δ/γ2 loop chimera ($\delta^{\gamma2}$). *E,* Cumulative probability distributions of confinement areas of synaptic and extrasynaptic δ subunits and δ/γ2 loop chimera. *F,* 25-75% interquartile range (IQR) and median confinement area of synaptic and extrasynaptic δ subunits and δ/γ2 loop chimera. *G,* Mean synaptic dwell times of δ subunits and δ/γ2 loop chimera. NS – not significant,*P<0.05, ***P<0.001. n = 226 – 11868. Box plots – KS test, Bar chart - two-tailed unpaired t-test.

Fig 6. Agonist-induced lateral diffusion of $GABA_A$Rs

A, Cumulative probability distributions of diffusion coefficients of synaptic α2 and α4 $GABA_A$Rs in control and +100 μM muscimol. *B,* Mean square displacement of synaptic α2 and α4 $GABA_A$Rs. *C,* 25-75% interquartile range (IQR) and median diffusion coefficient of synaptic α2 and α4 $GABA_A$Rs in control (C) and muscimol (M). *D,* Cumulative probability distributions of confinement areas of synaptic α2 and α4 $GABA_A$Rs. *E,* 25-75% interquartile range (IQR) and median confinement area of synaptic α2 and α4 $GABA_A$Rs. *F,* Cumulative probability

distributions of diffusion coefficients of extrasynaptic α2 and α4 $GABA_A$Rs in control and +100 μM muscimol. *G,* Mean square displacement of extrasynaptic α2 and α4 $GABA_A$Rs. *H,* 25-75% interquartile range (IQR) and median diffusion coefficient of extrasynaptic α2 and α4 $GABA_A$Rs in control and muscimol. *I,* Cumulative probability distributions of confinement areas of extrasynaptic α2 and α4 $GABA_A$Rs. *J,* 25-75% interquartile range (IQR) and median confinement area of extrasynaptic α2 and α4 $GABA_A$Rs. NS – not significant, ***P<0.001, KS test, n = 131 – 7599.

References

Alldred, M.J., Mulder-Rosi, J., Lingenfelter, S.E., Chen, G., Luscher, B., 2005. Distinct γ2 subunit domains mediate clustering and synaptic function of postsynaptic $GABA_A$ receptors and gephyrin. J. Neurosci. 25, 594–603.

Bannai, H., Levi, S., Schweizer, C., Dahan, M., Triller, A., 2006. Imaging the lateral diffusion of membrane molecules with quantum dots. Nat Protoc. 1, 2628–2634.

Bannai, H., Levi, S., Schweizer, C., Inoue, T., Launey, T., Racine, V., Sibarita, J.B., Mikoshiba, K., Triller, A., 2009. Activity-dependent tuning of inhibitory neurotransmission based on $GABA_A$R diffusion dynamics. Neuron 62, 670–682.

Bogdanov, Y., Michels, G., Armstrong-Gold, C., Haydon, P.G., Lindstrom, J., Pangalos, M., Moss, S.J., 2006. Synaptic $GABA_A$ receptors are directly recruited from their extrasynaptic counterparts. EMBO J. 25, 4381–4389.

Borgdorff, A.J., Choquet, D., 2002. Regulation of AMPA receptor lateral movements. Nature 417, 649–653.

Braat, S., Kooy, R.F., 2015. The $GABA_A$Receptor as a Therapeutic Target for Neurodevelopmental Disorders. Neuron. 86, 1119-30

Brady, M.L., Jacob, T.C., 2015. Synaptic localization of α5 GABA (A) receptors via gephyrin interaction regulates dendritic outgrowth and spine maturation. Dev. Neurobiol. 75, 1241-51

Brickley, S.G., Mody, I., 2012. Extrasynaptic $GABA_A$ Receptors: Their Function in the CNS and Implications for Disease. Neuron 73, 23–34.

Burli, T., Baer, K., Ewers, H., Sidler, C., Fuhrer, C., Fritschy, J.M., 2010. Single particle tracking

of α7 nicotinic AChR in hippocampal neurons reveals regulated confinement at glutamatergic and GABAergic perisynaptic sites. PLoS.One. 5, e11507.

Caraiscos, V.B., Elliott, E.M., You, T., Cheng, V.Y., Belelli, D., Newell, J.G., Jackson, M.F., Lambert, J.J., Rosahl, T.W., Wafford, K.A., MacDonald, J.F., Orser, B.A., 2004. Tonic inhibition in mouse hippocampal CA1 pyramidal neurons is mediated by α5 subunit-containing γ-aminobutyric acid type A receptors. Proc. Natl. Acad. Sci. U.S.A 101, 3662–3667.

Chandra, D., Jia, F., Liang, J., Peng, Z., Suryanarayanan, A., Werner, D.F., Spigelman, I., Houser, C.R., Olsen, R.W., Harrison, N.L., Homanics, G.E., 2006. $GABA_A$ receptor α4 subunits mediate extrasynaptic inhibition in thalamus and dentate gyrus and the action of gaboxadol. Proc. Natl. Acad. Sci. U.S.A 103, 15230–15235.

Choquet, D., Triller, A., 2013. The dynamic synapse. Neuron 80, 691–703.

Connolly, C.N., Kittler, J.T., Thomas, P., Uren, J.M., Brandon, N.J., Smart, T.G., Moss, S.J., 1999. Cell surface stability of γ-aminobutyric acid type A receptors. Dependence on protein kinase C activity and subunit composition. J.Biol.Chem. 274, 36565–36572.

Davenport, E.C., Pendolino, V., Kontou, G., McGee, T.P., Sheehan, D.F., López-Doménech, G., Farrant, M., Kittler, J.T., 2017. An Essential Role for the Tetraspanin LHFPL4 in the Cell-Type-Specific Targeting and Clustering of Synaptic $GABA_A$ Receptors. Cell Rep. 21, 70-83. https://doi.org/10.1016/j.celrep.2017.09.025

de Luca, E., Ravasenga, T., Petrini, E.M., Polenghi, A., Nieus, T., Guazzi, S., Barberis, A., 2017. Inter-Synaptic Lateral Diffusion of $GABA_A$ Receptors Shapes Inhibitory Synaptic Currents. Neuron 95, 63–69.e5.

Durkin, E.J., Muessig, L., Herlt, T., Lumb, M.J., Patel, R., Thomas, P., Bright, D.P., Jurd, R., Moss, S.J., Dickenson, A.H., Cacucci, F., Smart, T.G., 2018. Brain neurosteroids are natural anxiolytics targeting α2 subunit γ-aminobutyric acid type-A receptors. BioRxiv 462457; doi: https://doi.org/10.1101/462457.

Essrich, C., Lorez, M., Benson, J.A., Fritschy, J.M., Luscher, B., 1998. Postsynaptic clustering of major $GABA_A$ receptor subtypes requires the γ2 subunit and gephyrin. Nat. Neurosci. 1, 563–571.

Fernandes, C.C., Berg, D.K., Gomez-Varela, D., 2010. Lateral Mobility of Nicotinic Acetylcholine Receptors on Neurons Is Determined by Receptor Composition, Local Domain, and Cell Type. J. Neurosci. 30, 8841–8851.

Gerrow, K., Triller, A., 2014. $GABA_A$ receptor subunit composition and competition at synapses are tuned by $GABA_B$ receptor activity. Mol. Cell. Neurosci. 60, 97–107.

Glykys, J., Mann, E.O., Mody, I., 2008. Which $GABA_A$ Receptor Subunits Are Necessary for Tonic Inhibition in the Hippocampus? J. Neurosci. 28, 1421–1426.

Glykys, J., Mody, I., 2007. Activation of $GABA_A$ Receptors: Views from Outside the Synaptic Cleft. Neuron 56, 763–770.

Glykys, J., Peng, Z., Chandra, D., Homanics, G.E., Houser, C.R., Mody, I., 2007. A new naturally occurring $GABA_A$ receptor subunit partnership with high sensitivity to ethanol. Nat Neurosci 10, 40–48.

Gouzer, G., Specht, C.G., Allain, L., Shinoe, T., Triller, A., 2014. Benzodiazepine-dependent stabilization of $GABA_A$ receptors at synapses. Mol. Cell. Neurosci. 63, 101–113.

Groc, L., Heine, M., Cognet, L., Brickley, K., Stephenson, F.A., Lounis, B., Choquet, D., 2004. Differential activity-dependent regulation of the lateral mobilities of AMPA and NMDA receptors. Nat.Neurosci. 7, 695–696.

Hannan, S., Gerrow, K., Triller, A., Smart, T.G., 2016. Phospho-dependent Accumulation of $GABA_B$Rs at Presynaptic Terminals after NMDAR Activation. Cell Rep. 16, 1962–1973. DOI: 10.1016/j.celrep.2016.07.021.

Hannan, S., Mortensen, M., Smart, T.G., 2015. Snake neurotoxin α-bungarotoxin is an antagonist at native $GABA_A$ receptors. Neuropharmacology 93, 28-40

Hannan, S., Smart, T.G., 2018. Cell surface expression of homomeric $GABA_A$ receptors depends on single residues in subunit transmembrane domains. J. Biol. Chem. 293, 13427–13439.

Hannan, S., Wilkins, M.E., Dehghani-Tafti, E., Thomas, P., Baddeley, S.M., Smart, T.G., 2011. γ-aminobutyric acid type B ($GABA_B$) receptor internalization is regulated by the R2 subunit. J. Biol. Chem. 286, 24324-35.

Hannan, S., Wilkins, M.E., Thomas, P., Smart, T.G., 2013. Tracking cell surface mobility of GPCRs using alpha-bungarotoxin-linked fluorophores. Methods Enzym. 521, 109–129.

Harel, M., Kasher, R., Nicolas, A., Guss, J.M., Balass, M., Fridkin, M., Smit, A.B., Brejc, K., Sixma, T.K., Katchalski-Katzir, E., Sussman, J.L., Fuchs, S., 2001. The binding site of acetylcholine receptor as visualized in the X-Ray structure of a complex between α-bungarotoxin and a mimotope peptide. Neuron 32, 265–275.

Hausrat, T.J., Muhia, M., Gerrow, K., Thomas, P., Hirdes, W., Tsukita, S., Heisler, F.F., Herich, L., Dubroqua, S., Breiden, P., Feldon, J., Schwarz, J.R., Yee, B.K., Smart, T.G., Triller, A., Kneussel, M., 2015. Radixin regulates synaptic $GABA_A$ receptor density and is essential for reversal learning and short-term memory. Nat. Commun. 6, 6872. DOI: 10.1038/ncomms7872.

Kasugai, Y., Swinny, J.D., Roberts, J.D., Dalezios, Y., Fukazawa, Y., Sieghart, W., Shigemoto, R., Somogyi, P., 2010. Quantitative localisation of synaptic and extrasynaptic $GABA_A$ receptor subunits on hippocampal pyramidal cells by freeze-fracture replica immunolabelling. Eur. J. Neurosci. 32, 1868–1888.

Kittler, J.T., Delmas, P., Jovanovic, J.N., Brown, D.A., Smart, T.G., Moss, S.J., 2000. Constitutive endocytosis of $GABA_A$ receptors by an association with the adaptin AP2 complex modulates inhibitory synaptic currents in hippocampal neurons. J. Neurosci. 20, 7972–7977.

Klausberger, T., Roberts, J.D., Somogyi, P., 2002. Cell type- and input-specific differences in the number and subtypes of synaptic $GABA_A$ receptors in the hippocampus. J Neurosci 22, 2513–2521.

Levi, S., 2004. Gephyrin Is Critical for Glycine Receptor Clustering But Not for the Formation of Functional GABAergic Synapses in Hippocampal Neurons. J. Neurosci. 24, 207–217.

Loebrich, S., Bahring, R., Katsuno, T., Tsukita, S., Kneussel, M., 2006. Activated radixin is essential for $GABA_A$ receptor α5 subunit anchoring at the actin cytoskeleton. EMBO J 25, 987–999.

Lorenz-Guertin, J.M., Jacob, T.C., 2018. GABA type-A receptor trafficking and the architecture of synaptic inhibition. Dev. Neurobiol. 78, 238-270

Luscher, B., Fuchs, T., Kilpatrick, C., 2011. $GABA_A$ Receptor Trafficking-Mediated Plasticity of Inhibitory Synapses. Neuron 70, 385–409.

Macdonald, R.L., Kang, J.Q., Gallagher, M.J., 2010. Mutations in $GABA_A$ receptor subunits associated with genetic epilepsies. J. Physiol. 588, 1861–1869.

McKernan, R.M., Quirk, K., Prince, R., Cox, P.A., Gillard, N.P., Ragan, C.I., Whiting, P., 1991. $GABA_A$ receptor subtypes immunopurified from rat brain with α subunit-specific antibodies have unique pharmacological properties. Neuron 7, 667-76

Mikasova, L., Groc, L., Choquet, D., Manzoni, O.J., 2008. Altered surface trafficking of presynaptic cannabinoid type 1 receptor in and out synaptic terminals parallels receptor desensitization. Proc. Natl. Acad. Sci. U.S.A 105, 18596–18601.

Mitchell, S.J., Silver, R.A., 2003. Shunting inhibition modulates neuronal gain during synaptic excitation. Neuron 38, 433–445.

Mortensen, M., Ebert, B., Wafford, K., Smart, T.G., 2010. Distinct activities of GABA agonists at synaptic- and extrasynaptic-type $GABA_A$ receptors. J.Physiol 588, 1251–1268.

Mortensen, M., Smart, T.G., 2006. Extrasynaptic αβ subunit $GABA_A$ receptors on rat hippocampal pyramidal neurons. J. Physiol. 577, 841–856.

Moss, S.J., Smart, T.G., 2001. Constructing inhibitory synapses. Nat. Rev. Neurosci. 2, 240–250.

Muir, J., Arancibia-Carcamo, I.L., MacAskill, A.F., Smith, K.R., Griffin, L.D., Kittler, J.T., 2010. NMDA receptors regulate $GABA_A$ receptor lateral mobility and clustering at inhibitory synapses through serine 327 on the 2 subunit. Proc. Natl. Acad. Sci. 107, 16679–16684.

Mukherjee, J., Kretschmannova, K., Gouzer, G., Maric, H.M., Ramsden, S., Tretter, V., Harvey, K., Davies, P.A., Triller, A., Schindelin, H., Moss, S.J., 2011. The Residence Time of $GABA_A$Rs at Inhibitory Synapses Is Determined by Direct Binding of the Receptor α1 Subunit to Gephyrin. J. Neurosci. 31, 14677–14687.

Nusser, Z., Sieghart, W., Benke, D., Fritschy, J.-M., Somogyi, P., 1996. Differential synaptic localization of two major γ-aminobutyric acid type A receptor α-subunits on hippocampal pyramidal cells. Proc. Natl. Acad. Sci. USA 93, 11939–11944.

Olsen, R.W., Sieghart, W., 2009. $GABA_A$ receptors: subtypes provide diversity of function and pharmacology. Neuropharmacology 56, 141–148.

Oyrer, J., Maljevic, S., Scheffer, I.E., Berkovic, S.F., Petrou, S., Reid, C.A., 2018. Ion Channels in Genetic Epilepsy: From Genes and Mechanisms to Disease-Targeted Therapies. Pharmacol. Rev. 70, 142–173.

Petrini, E.M., Marchionni, I., Zacchi, P., Sieghart, W., Cherubini, E., 2004. Clustering of extrasynaptic $GABA_A$ receptors modulates tonic inhibition in cultured hippocampal neurons. J. Biol. Chem. 279, 45833–45843.

Prenosil, G.A., Schneider Gasser, E.M., Rudolph, U., Keist, R., Fritschy, J.M., Vogt, K.E., 2006. Specific subtypes of $GABA_A$ receptors mediate phasic and tonic forms of inhibition in hippocampal pyramidal neurons. J. Neurophysiol. 96, 846–857.

Renner, M., Choquet, D., Triller, A., 2009. Control of the postsynaptic membrane viscosity. J.Neurosci. 29, 2926–2937.

Renner, M., Schweizer, C., Bannai, H., Triller, A., Lévi, S., 2012. Diffusion barriers constrain receptors at synapses. PLoS ONE 7(8): e43032. https://doi.org/10.1371/journal.pone.0043032

Rudolph, U., Mohler, H., 2014. $GABA_A$ Receptor Subtypes: Therapeutic Potential in Down Syndrome, Affective Disorders, Schizophrenia, and Autism. Annu. Rev. Pharmacol. Toxicol. 54, 483–507.

Schmidt, M.J., Mirnics, K., 2015. Neurodevelopment, GABA System Dysfunction, and Schizophrenia. Neuropsychopharmacology 40, 190–206.

Serwanski, D.R., Miralles, C.P., Christie, S.B., Mehta, A.K., Li, X., De Blas, A.L., 2006. Synaptic and nonsynaptic localization of $GABA_A$ receptors containing the α5 subunit in the rat brain. J. Comp. Neurol. 499, 458-470

Sieghart, W., Sperk, G., 2002. Subunit composition, distribution and function of $GABA_A$ receptor subtypes. Curr. Top. Med. Chem. 2, 795–816.

Smart, T.G., 2015. $GABA_A$ Receptors, in: Zhang, J., Trudeau, M. (Eds.), Handbook of Ion Channels. pp. 345–359.

Stell, B.M., Brickley, S.G., Tang, C.Y., Farrant, M., Mody, I., 2003. Neuroactive steroids reduce neuronal excitability by selectively enhancing tonic inhibition mediated by δ subunit-containing $GABA_A$ receptors. Proc. Natl. Acad. Sci. U.S.A 100, 14439–14444

Sun, C., Sieghart, W., Kapur, J., 2004. Distribution of α1, α4, γ2, and δ subunits of $GABA_A$ receptors in hippocampal granule cells. Brain Res. 1029, 207–216.

Sun, M.-Y., Shu, H.-J., Benz, A., Bracamontes, J., Akk, G., Zorumski, C.F., Steinbach, J.H., Mennerick, S.J., 2018. Chemogenetic Isolation Reveals Synaptic Contribution of δ $GABA_A$ Receptors in Mouse Dentate Granule Neurons. J. Neurosci. 38, 8128-8145

Thomas, P., Mortensen, M., Hosie, A.M., Smart, T.G., 2005. Dynamic mobility of functional $GABA_A$ receptors at inhibitory synapses. Nat. Neurosci. 8, 889–897.

Tyagarajan, S.K., Fritschy, J.M., 2014. Gephyrin: a master regulator of neuronal function? Nat. Rev. Neurosci. 15, 141–156.

Uezu, A., Kanak, D.J., Bradshaw, T.W.A., Soderblom, E.J., Catavero, C.M., Burette, A.C., Weinberg, R.J., Soderling, S.H., 2016. Identification of an elaborate complex mediating postsynaptic inhibition. Science 353, 1123–1129.

Van Den Ent, F., Löwe, J., 2006. RF cloning: A restriction-free method for inserting target genes into plasmids. J. Biochem. Biophys. Methods 67, 67–74.

Wlodarczyk, A.I., Sylantyev, S., Herd, M.B., Kersante, F., Lambert, J.J., Rusakov, D.A., Linthorst, A.C.E., Semyanov, A., Belelli, D., Pavlov, I., Walker, M.C., 2013. GABA-Independent $GABA_A$ Receptor Openings Maintain Tonic Currents. J. Neurosci. 33, 3905-14

Yamasaki, T., Hoyos-Ramirez, E., Martenson, J.S., Morimoto-Tomita, M., Tomita, S., 2017. GARLH Family Proteins Stabilize $GABA_A$ Receptors at Synapses. Neuron 93, 1138–1152.e6.

Zarnowska, E.D., Keist, R., Rudolph, U., Pearce, R.A., 2009. Receptor α5 Subunits Contribute to $GABA_A$ slow Synaptic Inhibition in Mouse Hippocampus. J. Neurophysiol. 101, 1179–1191.

Zheleznova, N., Sedelnikova, A., Weiss, D.S., 2008. α1β2δ, a silent $GABA_A$ receptor: recruitment by tracazolate and neurosteroids. Br J Pharmacol 153, 1062–1071.

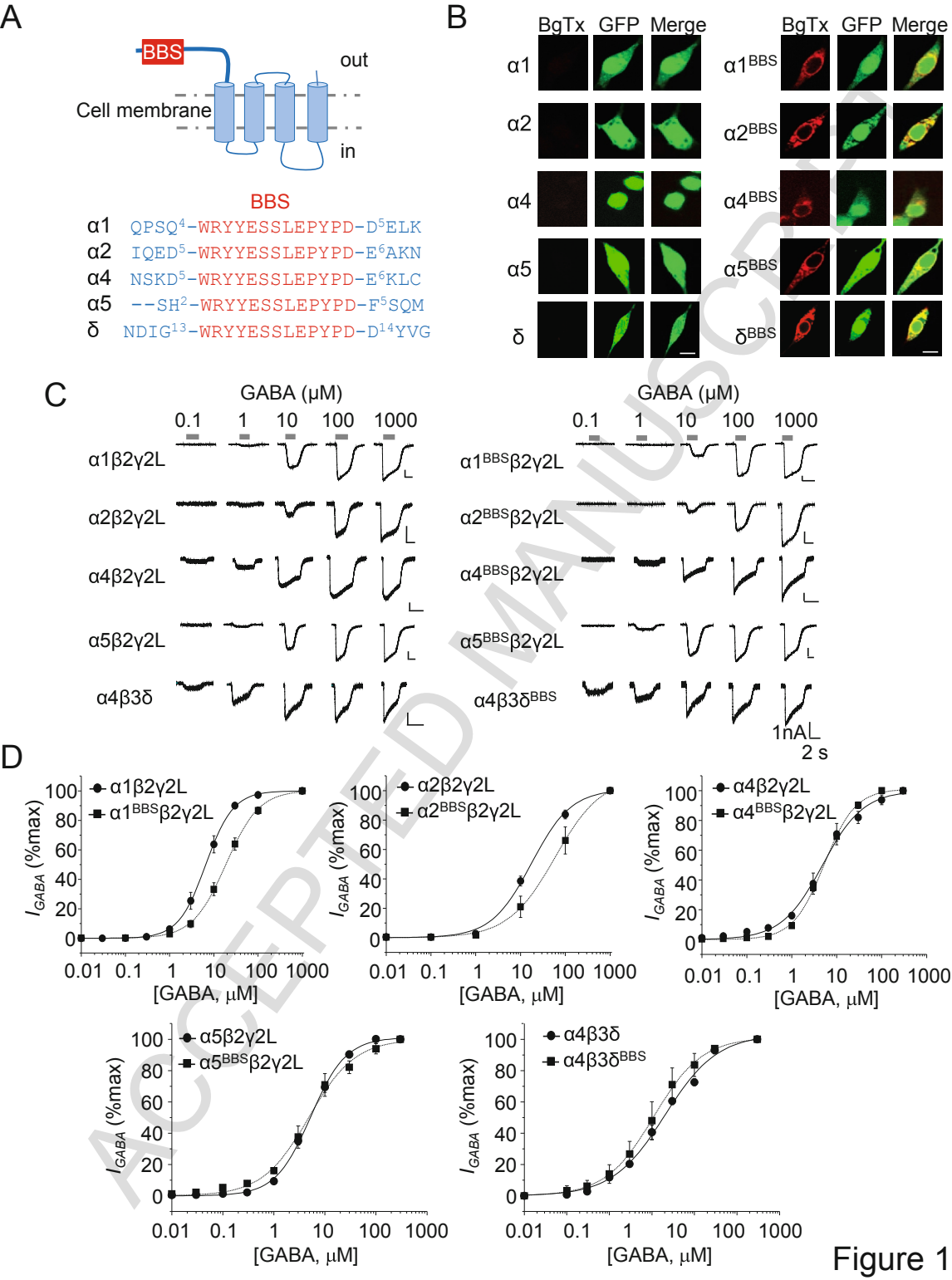

Figure 1

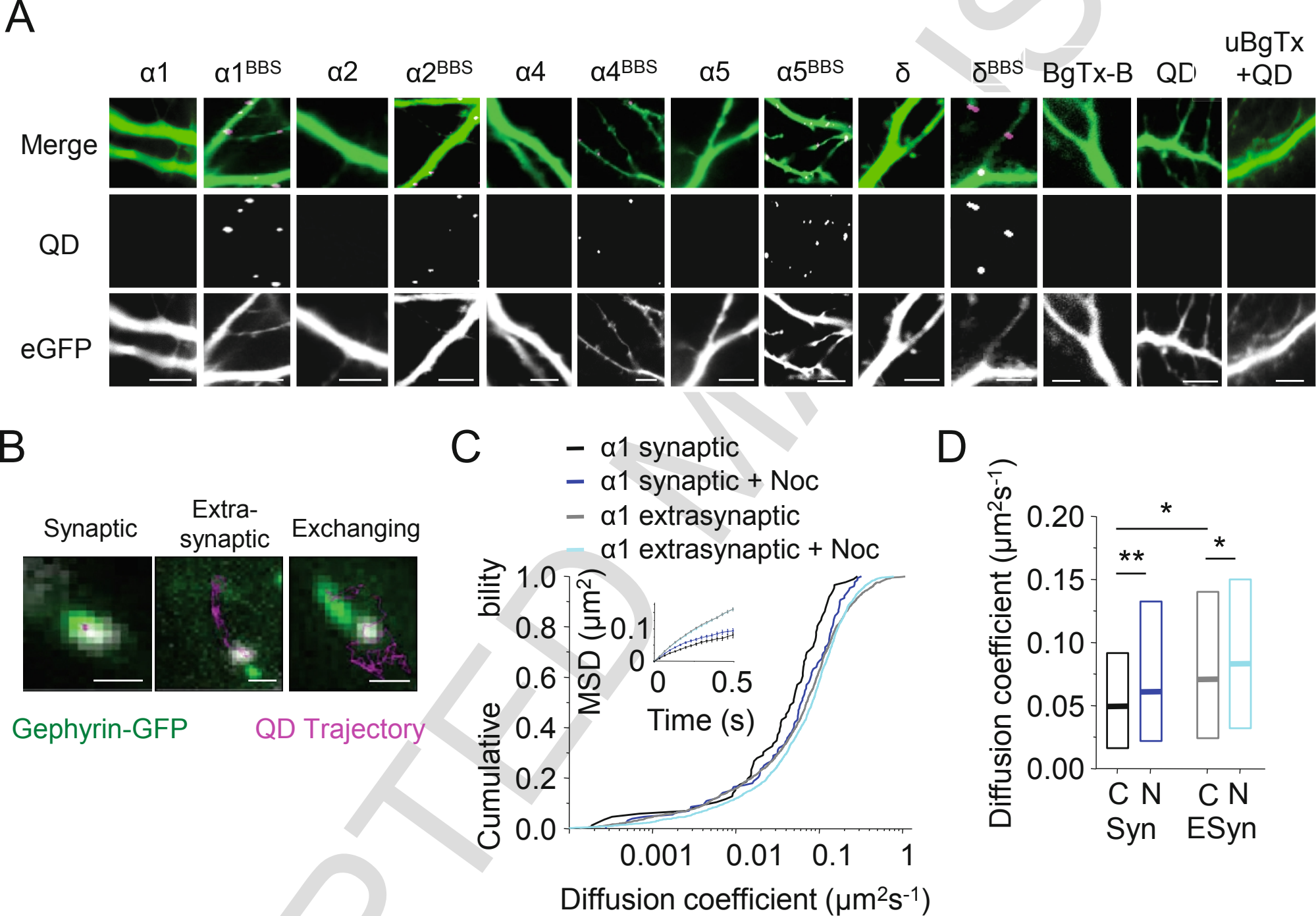
A
α1
α1BBS
α2
α2BBS
α4
α4BBS
α5
α5BBS
δ
δBBS
BgTx-B
QD
uBgTx +QD
Merge
QD
eGFP
B
Synaptic
Extra-synaptic
Exchanging
Gephyrin-GFP
QD Trajectory
C
α1 synaptic
α1 synaptic + Noc
α1 extrasynaptic
α1 extrasynaptic + Noc
Cumulative
bility
1.0
0.8
0.6
0.4
0.2
0.0
MSD (μm²)
0.1
0
0
0.5
Time (s)
0.001
0.01
0.1
1
Diffusion coefficient (μm²s⁻¹)
D
Diffusion coefficient (μm²s⁻¹)
0.20
0.15
0.10
0.05
0.00
*
**
*
C N
Syn
C N
ESyn

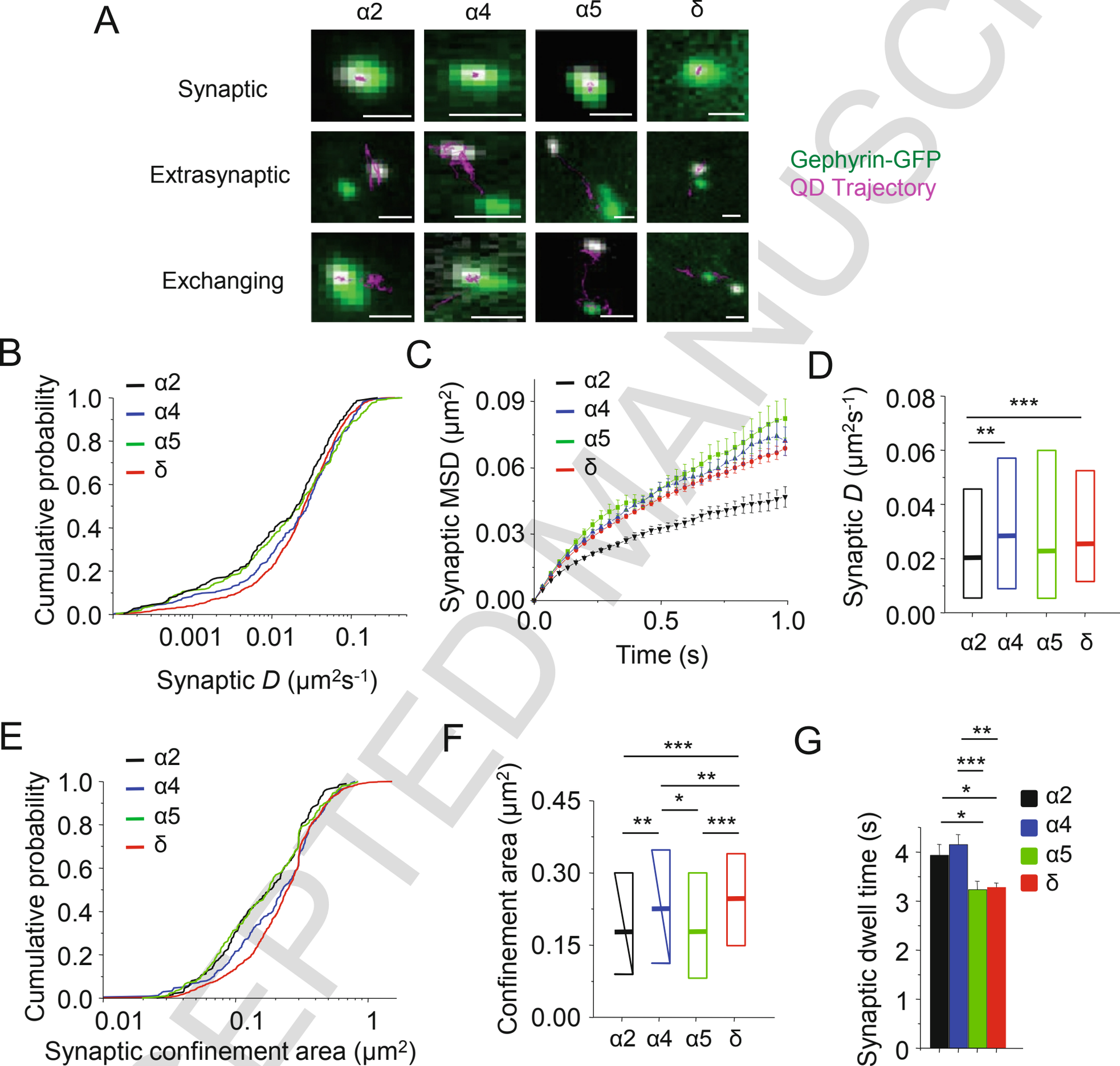

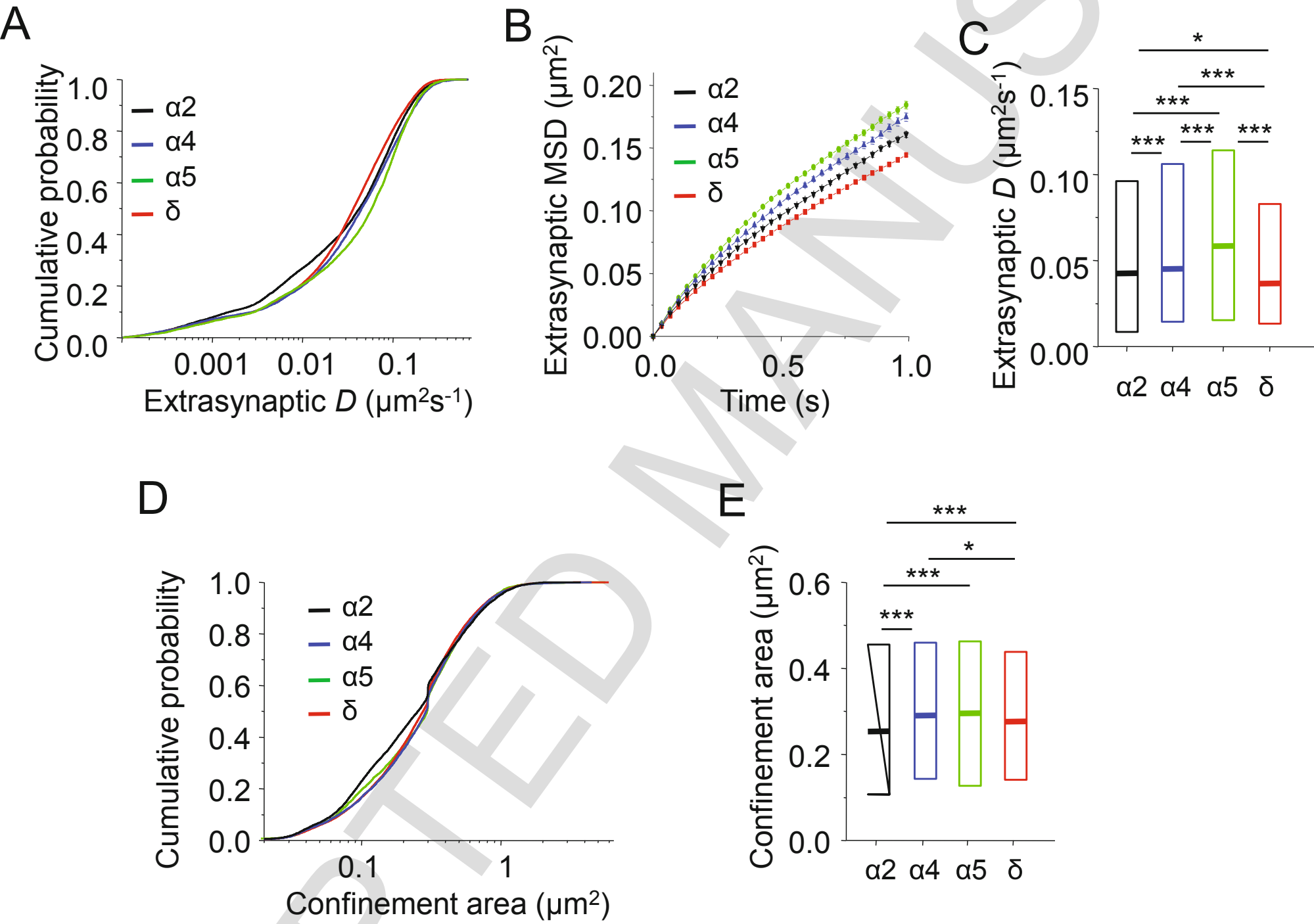

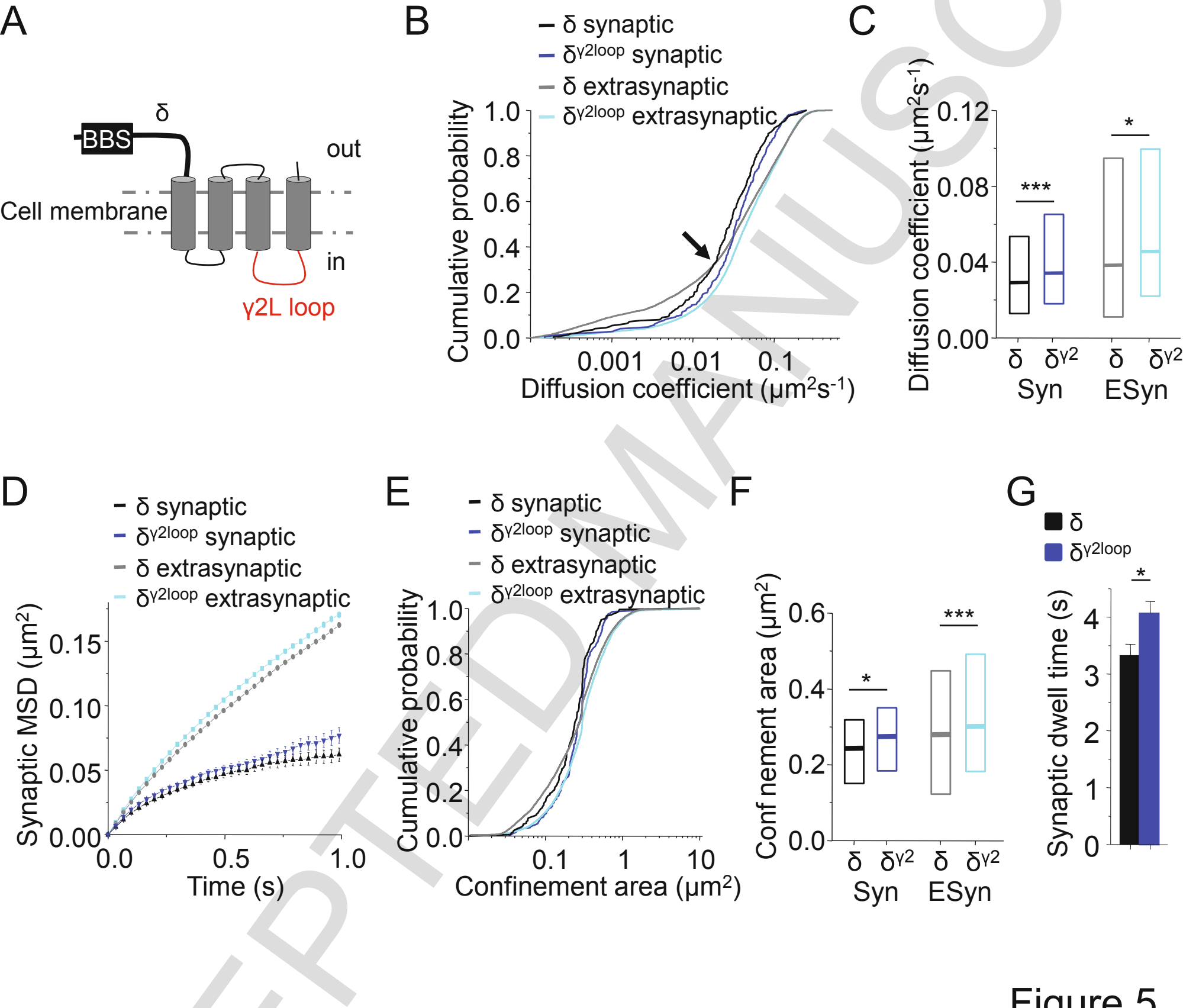
A
δ
BBS
out
Cell membrane
in
γ2L loop
B
δ synaptic
δγ2loop synaptic
δ extrasynaptic
δγ2loop extrasynaptic
Cumulative probability
1.0
0.8
0.6
0.4
0.2
0.0
0.001
0.01
0.1
Diffusion coefficient (μm²s⁻¹)
C
Diffusion coefficient (μm²s⁻¹)
0.12
0.08
0.04
0.00
***
*
δ
δγ2
δ
δγ2
Syn
ESyn
D
δ synaptic
δγ2loop synaptic
δ extrasynaptic
δγ2loop extrasynaptic
Synaptic MSD (μm²)
0.15
0.10
0.05
0.00
0.0
0.5
1.0
Time (s)
E
δ synaptic
δγ2loop synaptic
δ extrasynaptic
δγ2loop extrasynaptic
Cumulative probability
1.0
0.8
0.6
0.4
0.2
0.0
0.1
1
10
Confinement area (μm²)
F
Conf nement area (μm²)
0.6
0.4
0.2
0.0
*
***
δ
δγ2
δ
δγ2
Syn
ESyn
G
δ
δγ2loop
*
Synaptic dwell time (s)
4
3
2
1
0

Figure 5